



## Approximate seismic-wave traveltimes in laterally varying, layered, weakly anisotropic media

Ivan Pšenčík\*, Véronique Farra† and Ekkehart Tessmer††

\*Institute of Geophysics, Acad. Sci. of Czech Republic, Boční II, 141 31 Praha 4, Czech Republic

†Institut de Physique du Globe de Paris, F-75005 Paris, France

††Institute of Geophysics, Bundesstr. 55, 20146 Hamburg, Germany

Copyright 2011, SBGf - Sociedade Brasileira de Geofísica.

This paper was prepared for presentation at the Twelfth International Congress of the Brazilian Geophysical Society, held in Rio de Janeiro, Brazil, August 15-18, 2011.

Contents of this paper were reviewed by the Technical Committee of the Twelfth International Congress of The Brazilian Geophysical Society and do not necessarily represent any position of the SBGf, its officers or members. Electronic reproduction or storage of any part of this paper for commercial purposes without the written consent of The Brazilian Geophysical Society is prohibited.

### Abstract

**We extend the applicability of approximate, but very efficient and highly accurate formulae for computing traveltimes of seismic P and S waves propagating in smooth inhomogeneous, weakly anisotropic media, to layered media. We illustrate the accuracy of these formulae in smooth media by the comparison of their results with results of the Fourier pseudospectral method. The formulae can find applications in migration and traveltime tomography.**

### Introduction

A useful byproduct of the first-order ray tracing (Pšenčík and Farra, 2005; Farra and Pšenčík, 2010a; Iversen et al, 2009) are approximate, but simple and quite accurate formulae for computing traveltimes of seismic waves propagating in inhomogeneous, weakly anisotropic media and even in media of moderate anisotropy. First-order ray tracing is a technique based on perturbation theory, in which deviations of anisotropy from isotropy are considered to be small quantities, used further in the perturbation procedure. The basic idea of the first-order ray tracing is to replace the exact Hamiltonian formed by an eigenvalue of the Christoffel matrix, which controls ray tracing and dynamic ray tracing equations, by its first-order counterpart.

For P waves, the first-order ray tracing provides directly first-order traveltimes. Traveltimes of second-order accuracy can be simply computed by quadratures along first-order rays (Pšenčík and Farra, 2005). The procedure is straightforward and fast.

The situation is more complicated in case of S waves. S waves in inhomogeneous, weakly anisotropic media are coupled. They are computed using coupling ray theory along common trajectories called common rays (Farra and Pšenčík, 2010a). In the first-order ray tracing approximation, ray tracing and dynamic ray tracing equations are controlled by the Hamiltonian formed by an average of the first-order approximations of the corresponding S-wave eigenvalues of the Christoffel

matrix. Traveltimes of separate S waves are obtained as the sum of the first-order traveltime calculated along the common ray and of the corrections obtained by quadratures calculated along the common ray. The corrections consist of two terms, one term correcting the first-order S-wave traveltime along the common ray, the other term controlling the S-wave separation.

Here the applicability of the above described traveltime formulae is extended to layered media. Equations for tracing first-order P-wave rays or first-order common S-wave rays are supplemented by a formula (Snell's law) for the determination of the first-order slowness vector of a selected generated wave. The generated wave may be reflected or transmitted P or common S waves.

The lower-case indices  $i, j, k, l, \dots$  take the values of 1,2,3, the upper-case indices  $I, J, K, L, \dots$  take the values of 1,2. The Einstein summation convention over repeated indices is used. The upper index  $[\mathcal{M}]$  is used to denote quantities related to the S-wave common ray.

### Traveltime computations in smooth media

The first-order P-wave ray or common S-wave ray in an inhomogeneous, weakly anisotropic medium can be obtained by solving the first-order ray tracing (FORT) equations:

$$\frac{dx_i}{d\tau} = \frac{1}{2} \frac{\partial G(x_m, p_m)}{\partial p_i}, \quad \frac{dp_i}{d\tau} = -\frac{1}{2} \frac{\partial G(x_m, p_m)}{\partial x_i}. \quad (1)$$

Here  $x_i$  and  $p_i$  are the Cartesian coordinates of the first-order P-wave or S-wave common ray and the components of the corresponding first-order slowness vectors, respectively. Parameter  $\tau$  is the first-order traveltime. Symbol  $G$  denotes either the first-order P-wave eigenvalue  $G^{[3]}(x_m, p_m)$  or the average of the first-order S-wave eigenvalues:

$$G^{[\mathcal{M}]}(x_m, p_m) = \frac{1}{2} (G^{[1]} + G^{[2]}). \quad (2)$$

The symbol  $G^{[3]}$  denotes the first-order approximation of the greatest eigenvalue and  $G^{[1]}$  and  $G^{[2]}$  in (2) the first-order approximations of two smaller eigenvalues of the generalized Christoffel matrix with elements  $\Gamma_{ik}$ :

$$\Gamma_{ik}(x_m, p_m) = a_{ijkl}(x_m) p_j p_l. \quad (3)$$

The fourth-order tensor  $a_{ijkl}$  is the tensor of density-normalized elastic moduli,

$$a_{ijkl} = c_{ijkl} / \rho, \quad (4)$$

$c_{ijkl}$  being elements of the fourth-order tensor of elastic moduli and  $\rho$  the density.

The initial conditions for the ray-tracing equations (1) for  $\tau = \tau_0$  read:

$$x_i(\tau_0) = x_i^0, \quad p_i(\tau_0) = p_i^0. \quad (5)$$

Here,  $x_i^0$  are the coordinates of source point  $\mathbf{x}^0$ , and  $p_i^0 = n_i^0/c_0$  are the components of the first-order slowness vector  $\mathbf{p}^0$  at the source. Symbol  $c_0$  denotes the first-order approximation of either P-wave or S-wave common phase velocity in the direction  $\mathbf{n}^0$  at source point  $\mathbf{x}^0$ .

Pšenčík and Farra (2005) offer second-order traveltimes formula for P waves, which reads

$$\tau_P(\tau, \tau_0) = \tau + \Delta\tau_P(\tau, \tau_0). \quad (6)$$

Here  $\tau$  denotes the first-order traveltimes obtained by integrating the ray tracing system (1) with  $G$  replaced by  $G^{[3]}$ . Symbol  $\Delta\tau_P$  denotes the second-order traveltimes correction:

$$\Delta\tau_P = -\frac{1}{2} \int_{\tau_0}^{\tau} \frac{B_{13}^2(\mathbf{p}^{[3]}) + B_{23}^2(\mathbf{p}^{[3]})}{1 - \frac{1}{2}[B_{11}(\mathbf{p}^{[3]}) + B_{22}(\mathbf{p}^{[3]})]} d\tau. \quad (7)$$

The traveltimes formulae for S waves are more complicated. If we assume that the common S-wave ray does not pass through a singularity, traveltimes of S1 and S2 waves,  $\tau_{S1,S2}$ , are given by the formula (Farra and Pšenčík, 2010a; see also Iversen et al., 2009):

$$\tau_{S1,S2}(\tau, \tau_0) = \tau^{[M]} + \Delta\tau_{S1,S2}(\tau, \tau_0). \quad (8)$$

Here  $\tau^{[M]}$  denotes the first-order traveltimes obtained by integrating (1) with  $G$  replaced by  $G^{[M]}$ , see (2). The term  $\Delta\tau_{S1,S2}$  is the traveltimes correction, which consists of two terms:

$$\Delta\tau_{S1,S2}(\tau, \tau_0) = \Delta\tau^{[M]}(\tau, \tau_0) + \Delta\tau_{S1,S2}^S(\tau, \tau_0). \quad (9)$$

The first term on the RHS of (9),  $\Delta\tau^{[M]}$ , is the second-order traveltimes correction along the common S-wave ray. It reads:

$$\Delta\tau^{[M]} = \frac{1}{4} \int_{\tau_0}^{\tau} \frac{B_{13}^2(\mathbf{p}^{[M]}) + B_{23}^2(\mathbf{p}^{[M]})}{B_{33}(\mathbf{p}^{[M]}) - 1} d\tau. \quad (10)$$

The second term in (9),  $\Delta\tau_{S1,S2}^S$ , is the term, which controls the separation of S waves, and it reads:

$$\Delta\tau_{S1,S2}^S = \pm \frac{1}{4} \int_{\tau_0}^{\tau} \sqrt{[M_{11}(\mathbf{p}^{[M]}) - M_{22}(\mathbf{p}^{[M]})]^2 + 4M_{12}^2(\mathbf{p}^{[M]})} d\tau. \quad (11)$$

The elements of the matrix  $\mathbf{M}(\mathbf{p}^{[M]})$  can be expressed in terms of the elements of the matrix  $\mathbf{B}$ :

$$M_{KL}(\mathbf{p}^{[M]}) = B_{KL}(\mathbf{p}^{[M]}) - \frac{B_{K3}(\mathbf{p}^{[M]})B_{L3}(\mathbf{p}^{[M]})}{B_{33}(\mathbf{p}^{[M]}) - 1}. \quad (12)$$

It remains to define the elements of the symmetric matrix  $\mathbf{B}$  appearing in (7), (10) and (12). They are given by the formula

$$B_{jl}(\mathbf{p}) = \Gamma_{ik}(\mathbf{p}) e_i^{[j]} e_k^{[l]}. \quad (13)$$

Symbols  $e_i^{[j]}$  in (13) denote the components of unit vectors  $\mathbf{e}^{[j]}$ . Vectors  $\mathbf{e}^{[1]}$  and  $\mathbf{e}^{[2]}$  are perpendicular to the third vector  $\mathbf{e}^{[3]}$  chosen so that  $\mathbf{e}^{[3]} = \mathbf{n}$ . Here  $\mathbf{n}$  is a unit vector specifying the direction of the first-order slowness vector  $\mathbf{p}$ . Vector  $\mathbf{e}^{[3]}$  can be determined from the second set of FORT equations (1). Note that the matrix  $\mathbf{B}$  is different along the P-wave ray ( $\mathbf{p} = \mathbf{p}^{[3]}$ ) and common S-wave ray ( $\mathbf{p} = \mathbf{p}^{[M]}$ ). Vectors  $\mathbf{e}^{[K]}$  can be chosen arbitrarily in the plane perpendicular to  $\mathbf{n}$  at any point of the first-order P-wave or common S-wave ray.

### Transformation of a slowness vector across an interface

Let us consider an interface  $\Sigma$  and either a P-wave ray or a common S-wave ray incident at interface  $\Sigma$ . The slowness vector of an arbitrarily generated wave can be written in the form (Farra and Pšenčík, 2010b)

$$\mathbf{p}^G = \mathbf{b} + \xi^G \mathbf{N} = \mathbf{p} - (\mathbf{p} \cdot \mathbf{N}) \mathbf{N} + \xi^G \mathbf{N}. \quad (14)$$

Here,  $\mathbf{p}$  and  $\mathbf{p}^G$  are first-order slowness vectors of the incident and generated ( $G$ ) waves,  $\mathbf{N}$  is the unit normal to interface  $\Sigma$  at the point of the incidence at  $\Sigma$ . The symbol  $\xi^G$  represents the scalar component of  $\mathbf{p}^G$  to  $\mathbf{N}$ , and  $\mathbf{b}$  represents the vectorial component of  $\mathbf{p}^G$ , tangential to  $\Sigma$ . Components  $\xi^G$  of any generated wave can be found from the first-order eikonal equations satisfied by the waves generated on corresponding sides of the interface:

$$G(\mathbf{b} + \xi^G \mathbf{N}) = 1. \quad (15)$$

To solve equation (15), we can use an iterative procedure proposed by Dehghan et al. (2007) and described in detail by Farra and Pšenčík (2010b). In it, we seek the first-order slowness vector  $\mathbf{p}^{G\{j\}}$  of a selected generated wave in the  $j$ -th iteration in the form

$$\mathbf{p}^{G\{j\}} = \mathbf{b} + \xi^{G\{j\}} \mathbf{N}, \quad (16)$$

where

$$\xi^{G\{j\}} = \xi^{G\{j-1\}} - \frac{G(\mathbf{p}^{G\{j-1\}}) - 1}{N_k \partial G / \partial p_k(\mathbf{p}^{G\{j-1\}})}. \quad (17)$$

The initial value of the quantity  $\xi^{G(0)}$  is determined for a reference isotropic medium. The explicit expressions for  $G$  and  $\partial G / \partial p_k$  can be found in papers on FORT, see more details in Farra and Pšenčík (2010b).

### Computation of traveltimes in layered media

The procedure of computing traveltimes of multiply reflected/transmitted, converted or unconverted waves is now as follows. Ray tracing equations (1) with  $G$  replaced by  $G^{[3]}$  if we wish to start with the P wave or by  $G^{[M]}$  if we wish to start with one of the S waves are solved with initial conditions (5). After reaching the first interface, the first-order slowness vector of the selected generated wave is determined from eq. (14), solving eq. (15). The coordinates of the point of incidence and the first-order slowness vector determined from eq. (14) can be used as initial conditions for solving ray tracing equations (1) along the ray of a generated wave. At the next interface, the procedure continues as described above. When tracing of the ray of multiply reflected wave is finished, formulae (6) or (8) are applied along individual elements of the ray, depending on the type of the wave considered along a considered element. Along a single common S-wave ray, we can get corresponding traveltimes of both S waves.

### Tests of accuracy of approximate traveltimes formulae

It was shown by Pšenčík and Farra (2005) that even for a model with P-wave anisotropy of about 20%, the relative error of the FORT P-wave traveltimes compared with the standard ray theory traveltimes is less than 1%. For a model with S-wave anisotropy of about 7% and for the S-wave separation of about 13% Iversen et al. (2009) found S-waves relative errors about 0.5% or less. Here we illustrate the accuracy of the above presented formulae by comparing obtained traveltimes with highly accurate synthetics computed with the code based on the Fourier method (FM), a pseudo-spectral method (see, e.g., Kosloff and Baysal, 1982). Traveltimes calculated from approximate formulae given above (coloured crosses) are compared with maxima of envelopes of signals used in the FM. In the following, we concentrate on S waves only. Similar tests with P waves give very accurate results.

We consider the VSP configuration with the source and the borehole situated in a vertical plane  $(x, z)$ , see the schematic illustration in Figure 1. The borehole is parallel to the  $z$  axis, and the vertical single-force source is located on the surface at  $z = 0$  km, at a distance of 1 km from the borehole.

First we compare results of the approximate traveltimes formulae and of the FM method in a model of vertically inhomogeneous weakly orthorhombic medium. It is a modified version (decreased anisotropy) of the model proposed by Schoenberg and Helbig (1997). We rotated the model by  $42.5^\circ$  around the vertical axis so that the waves propagating to the profile of receivers pass close to the conical singularity. By this, we want to show that the formulae work safely even in vicinities of singularities. We consider 38 receivers distributed uniformly along the borehole situated in the  $(x, z)$  plane, starting from  $z = 0.04$  km with steps of 0.04 km. The variations of the S-wave phase velocities in the  $(x, z)$  plane for the orthorhombic model are shown in Figure 2. Figure 3 shows the comparison of traveltimes computed with formulae presented above (faster S wave blue, slower red) and synthetics of the transverse component of the displacement vector computed by the FM method. The fit of approximate traveltimes with the FM synthetics is very good.

Next we consider a model with stronger anisotropy and separation of S waves, proposed by Bulant and Klimeš (2008). This model represents a limit of applicability of the proposed approximate traveltimes formulae. We consider 29 receivers distributed uniformly along the borehole situated in the  $(x, z)$  plane, starting from  $z = 0.01$  km with the step of 0.02 km. The model is vertically inhomogeneous, transversely isotropic with a horizontal axis of symmetry (HTI). The axis of symmetry is rotated counterclockwise everywhere in the plane  $(x, y)$  by  $45^\circ$  from the  $x$ -axis. The variations of the S-wave phase velocities in the  $(x, z)$  plane for the HTI model are shown in Figure 4. The left-hand plot corresponds to a depth of  $z = 0$  km, the right-hand plot to a depth of  $z = 1$  km. Velocities are shown as functions of the angle of propagation. They vary from  $0^\circ$  (horizontal propagation) to  $90^\circ$  (vertical propagation). Figure 5 shows the comparison of traveltimes computed with formulae presented above (faster S wave blue, slower red) and synthetics of the transverse component

of the displacement vector computed by the FM method. Although the separation of waves is large and the applicability of the approximate formulae is on its limit, the fit is relatively good.

### Summary and Conclusions

By comparison of results of recently developed approximate traveltimes formulae with synthetics generated by the code based on the Fourier pseudospectral method we illustrated high accuracy of the approximate formulae. We extended their applicability to laterally varying layered, weakly anisotropic media. We plan to test their accuracy for unconverted and converted P and S waves in the way we tested their accuracy in smooth media.

Previous tests and tests presented in this contribution indicate that the accuracy of the approximate formulae is very high. Their use is also very efficient, especially when S waves are considered. For calculating traveltimes of both S waves, it is sufficient to trace just one common S-wave ray. When supplemented by the first-order dynamic ray tracing, the procedure offers various versions of very efficient two-point ray tracing. The formulae can find applications, for example, in migration and traveltimes tomography.

### References

- Bulant, P. and Klimeš, L., 2008, Numerical comparison of the isotropic-common-ray and anisotropic-common-ray approximations of the coupling ray theory: *Geophys. J. Int.*, Vol. 175, 357–374.
- Dehghan, K., Farra, V. and Nicolétis, L., 2007, Approximate ray tracing for qP-waves in inhomogeneous layered media with weak structural anisotropy: *Geophysics*, Vol. 72, No. 5, pSM47–SM60.
- Farra, V. and Pšenčík, I., 2010a, Coupled S waves in inhomogeneous weakly anisotropic media using first-order ray tracing: *Geophys.J.Int.*, Vol. 180, 405–417.
- Farra, V. and Pšenčík, I., 2010b, First-order reflection/transmission coefficients for unconverted plane P waves in weakly anisotropic media: *Geophys.J.Int.*, Vol. 183, 1443–1454.
- Iversen, E., Farra, V. and Pšenčík, I., 2009, Shear-wave traveltimes in inhomogeneous weakly anisotropic media: 79th Ann. Internat. Mtg., Soc. Expl. Geophys., Expanded Abstracts 28, 3486-3490, doi:10.1190/1.3255587.
- Kosloff, D. and Baysal, E., 1982, Forward modeling by a Fourier method: *Geophysics*, Vol. 47, 1402–1412.
- Pšenčík, I., and Farra, V., 2005, First-order ray tracing for qP waves in inhomogeneous weakly anisotropic media: *Geophysics*, Vol. 70, No. 6, pD65–D75.
- Schoenberg, M. and Helbig, K., 1997, Orthorhombic media: Modeling elastic wave behavior in a vertically fractured earth: *Geophysics*, Vol. 62, 1954–1974.

**Acknowledgments**

A substantial part of this work was done during IP's stay at the IPG Paris at the invitation of the IPGP. We are grateful to the Consortium Project "Seismic waves in complex 3-D structures" (SW3D) and Research Project 210/11/0117 of the Grant Agency of the Czech Republic for support.

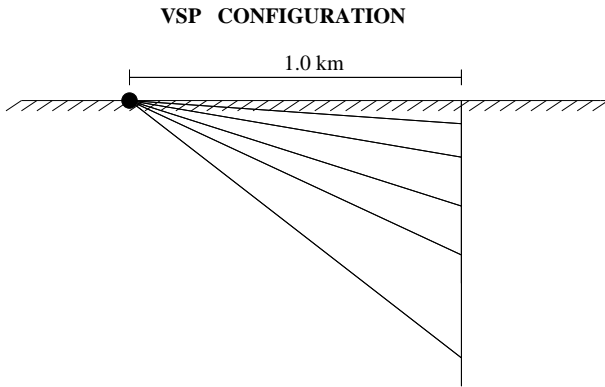


Figure 1: A schematic illustration of the VSP geometry used for the computations.

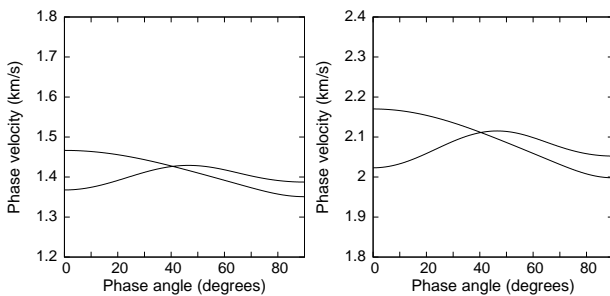


Figure 2: The S-wave phase-velocity sections in the  $(x, z)$  plane for the orthorhombic model. The velocities vary from the horizontal ( $0^\circ$ ) to the vertical ( $90^\circ$ ) direction of the wave normal. Left- and right-hand plots correspond to  $z = 0$  km and  $z = 3$  km, respectively.

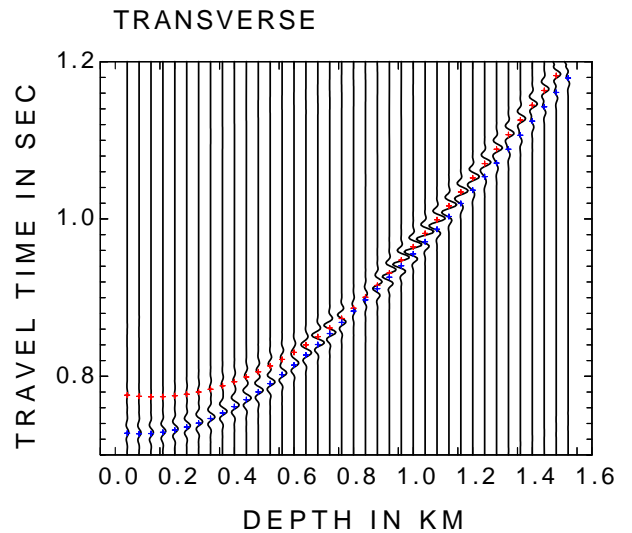


Figure 3: Comparison of the FM seismograms generated by the vertical single-force source in the orthorhombic model and traveltimes of faster (blue) and slower (red) S waves computed with presented approximate formulae.

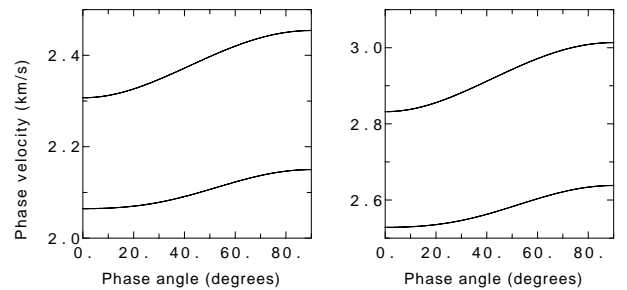


Figure 4: The S-wave phase-velocity sections in the  $(x, z)$  plane for the HTI model. The velocities vary from the horizontal ( $0^\circ$ ) to the vertical ( $90^\circ$ ) direction of the wave normal. Left- and right-hand plots correspond to  $z = 0$  km and  $z = 1$  km, respectively.

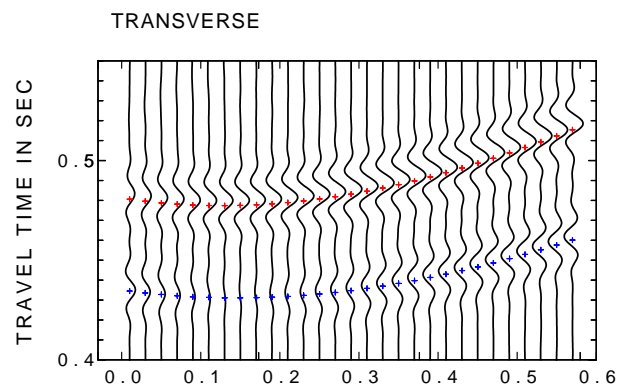


Figure 5: Comparison of the FM seismograms generated by the vertical single-force source in the HTI model and traveltimes of faster (blue) and slower (red) S waves computed with presented approximate formulae.